

# Photoionization spectroscopy in AlGaIn/GaN high electron mobility transistors

P. B. Klein<sup>a)</sup>

Naval Research Laboratory, Washington, DC 20375-5347

(Received 4 February 2002; accepted 2 August 2002)

A model is developed to describe the light-induced restoration of the drain current from current collapse in AlGaIn/GaN high electron mobility transistors. The model assumes that the collapse results from a transfer at large drain bias of hot carriers from the gate–drain region of the two-dimensional electron gas to deep traps in the high-resistivity GaN layer. Application of the model provides a means of determining the photoionization cross sections and the areal densities of the responsible traps. Where multiple trapping species are involved, it is shown that photoinduced transitions between trapping sites can significantly alter the response of the drain current to light illumination, and must therefore be taken into account. [DOI: 10.1063/1.1510564]

## I. INTRODUCTION

Nitride-based electronic devices are of great current interest because of their potential to operate at high power, high temperature, and high frequency. While excellent output characteristics have been reported,<sup>1,2</sup> these results are not always reproducible, due to the presence of deep trapping centers that occur within the device structures.<sup>3</sup> These defects can trap mobile charge, leading to a number of possible effects which are deleterious to device performance. A trapping phenomenon of particular concern is current collapse. When a high drain–source voltage is applied to a field effect transistor (FET), hot channel carriers can be injected into neighboring regions of the device containing a high concentration of deep traps. These carriers can be trapped and can remain trapped after the drain bias is removed, thus leading to current collapse — a sustained reduction in the dc drain current and an increase in the knee voltage. This results in a corresponding reduction in the output power of the device. Consequently, identification of the deep traps responsible for this effect is currently of great interest.

It is noteworthy that current collapse, historically an effect on the dc current–voltage ( $I$ – $V$ ) characteristic,<sup>3,4</sup> is not the same effect recently reported using the same terminology, but referring to the reduction of the device output power at microwave frequencies.<sup>5,6</sup> Although the dc effect will have an influence on the output power at high frequencies, other defect-related phenomena, such as gate lag (usually associated with surface states), specifically affects the high frequency device performance.

We have recently introduced an experimental technique, photoionization spectroscopy,<sup>7</sup> that probes the traps causing current collapse directly. These measurements take advantage of the fact that trapped carriers can be released from the filled traps (thus restoring the drain current) by the absorption of light. The spectral dependence of this absorption-photoionization spectrum — is characteristic of a deep cen-

ter, and can be employed as a signature of the relevant trap. Measurement of the spectral dependence of this light-induced drain current increase in a GaN metal–semiconductor FET (MESFET) was shown<sup>7,8</sup> to generate an absorption spectrum reflecting the existence of two distinct trap species. These results have been recently verified independently by other workers.<sup>9,10</sup> The two traps, which are responsible for current collapse in the GaN MESFET, were found to be located in the high resistivity (HR) GaN buffer layer. Photoionization spectroscopy measurements of current collapse in AlGaIn/GaN high electron mobility transistors (HEMTs) revealed similar spectra,<sup>11</sup> indicating that the same HR-GaN traps cause collapse in these devices as well. An example of such spectra for the MESFET and HEMT structures, reproduced from Ref. 12, are shown in Fig. 1.

While these measurements provide a spectroscopic “fingerprint” of the traps involved in current collapse and some indication of their depth, it is desirable to obtain a more quantitative characterization of the traps. In the case of the GaN MESFET, this was accomplished by measuring the dependence of the light-induced drain current increase in the collapsed device as a function of the amount of incident light illumination. These light illumination studies were fitted<sup>8</sup> with a model for the drain current increase in which the photoexcited carriers drift back to the conducting channel (under the influence of the electric field produced by the original transfer of charge into the HR-GaN layer), thus reducing the channel depletion region at the channel/HR-GaN interface and increasing the collapsed drain current. The analysis using this procedure enabled the determination of areal trap concentrations and photoionization cross sections for the two traps.

For the case of the AlGaIn/GaN HEMT structure, light illumination studies and the fitted trap characteristics have been reported in a recent letter (Ref. 13). Because of the differences in the nature of the two structures, the model employed to extract trap concentrations from light illumination measurements in the MESFET is not directly applicable to similar measurements in the HEMT. Consequently, a separate model was developed for the HEMT structure. In this

<sup>a)</sup>Electronic mail: klein@bloch.nrl.navy.mil

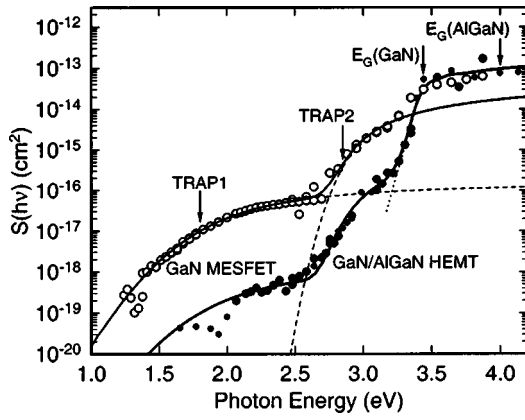


FIG. 1. Photoionization spectra reported in Ref. 12 of a GaN MESFET and an AlGaN/GaN HEMT structure. Two below-gap absorptions are associated with the two deep traps that are responsible for current collapse in these devices. The absorption threshold energies were found to be at 1.8 and 2.85 eV.

work we describe in detail the model employed to determine the HEMT trap characteristics. Some previously reported experimental data are included here in order to provide necessary background information for the discussion of the model.

## II. PHOTOIONIZATION MODEL

As a result of current collapse, a significant fraction of the sheet charge in the high-field region of the two-dimensional electron gas (2DEG) between the gate and drain can be transferred from the channel due to hot electron injection and subsequent trapping. The resistance associated with this portion of the 2DEG channel increases accordingly, and can dominate the total channel resistance when the device is fully collapsed. Then, for subsequent measurements (within the linear region of the  $I-V$  curve) the drain current becomes proportional to the sheet charge  $n_s$  in this region.<sup>14</sup> While this approximation begins to break down once the incident light has restored most of the collapsed drain current, this simple approach still provides a useful method for analyzing light illumination measurements in HEMT structures.

Light illumination studies measure the increase of the drain current in a fully collapsed device due to illumination by a measured amount of monochromatic light. These studies provide a measure of the fractional increase in the drain current induced by the light, relative to the collapsed drain current (measured in the dark), as a function of the total amount of light incident on the device.<sup>8</sup> The fractional current increase,  $[I(h\nu) - I_{\text{dark}}]/I_{\text{dark}} \equiv \Delta I/I_{\text{dark}}$ , reflects the fraction of filled traps that are emptied by the light, and is related to the trap photoionization cross section. When a large drain-source bias is applied to the device, hot 2DEG carriers are injected into the HR GaN, where they are trapped. This results in a reduction in  $n_s$  by an amount equal to the areal density of traps filled due to the hot carrier injection. The initial drain current, measured before the application of the high voltage, is written in the form

$$I_d = A n_s, \tag{1}$$

while the ‘‘collapsed’’ drain current, measured in the dark is

$$I_{\text{dark}} = A(1 - \beta)n_s, \tag{2}$$

where  $\beta$  is the fraction of the original sheet charge that was trapped at deep defects.

It is evident from Fig. 1 that the carriers can be trapped by more than one species of deep trap that is empty before the high voltage is applied. If there are  $N$  species of such traps, each having a total concentration  $n_{j,0}$  ( $j = 1 - N$ ), and all of the traps are filled after the application of a high drain bias, then the total filled trap concentration existing before light illumination is given by

$$n_{T(\text{DARK})}^- = \sum_{j=1}^N n_{j,0} \equiv \sum_{j=1}^N \beta_j \cdot n_s, \tag{3}$$

where  $\beta_j$  is the fraction of the original sheet charge trapped on trap species  $j$ , and  $\beta$  as defined above is therefore given by  $\beta = \sum_{j=1}^N \beta_j$ .

After the traps have been filled, if monochromatic light of photon energy  $h\nu$  and incident photon flux  $\Phi$  illuminates the device for a time  $t$ , trapped carriers will be photoionized from the filled traps and will return to the 2DEG to restore the drain current. As a result, the areal concentration of filled traps of species  $j$  will be reduced from  $n_{j,0}$ , its initial value, to  $n_j^-(t)$ . Here the superscript emphasizes that the trap is filled: We denote the concentrations of filled and empty traps by  $n_j^-$  and  $n_j^o$ , respectively. Since a given trap is either filled or empty, we also have  $n_{j,0} = n_j^-(t) + n_j^o(t)$ .

For convenience, the absorption threshold energies  $E_j$  of the  $N$  trap species will be assumed to increase monotonically with the index  $j$ . Then, only  $k$  species of traps with photoionization thresholds less than  $h\nu$  (corresponding to  $j \leq k$ ) will contribute to the drain current restoration. The remaining traps ( $k < j \leq N$ ) with higher thresholds will remain filled, and the drain current can be only partially restored.

Since the increase  $\Delta n_s$  in the 2DEG sheet charge due to light illumination is equal to the light-induced loss in the areal density of trapped charge,  $\Delta n_s$  can be written, as a function of illumination time and incident photon flux  $\Phi$ , as

$$\Delta n_s(\Phi, t) = \sum_{j=1}^k [n_{j,0} - n_j^-(\Phi, t)]. \tag{4}$$

The fractional increase in the drain current above the collapsed level, induced by incident light of fixed photon energy  $h\nu$ , is then determined [using Eqs. (1), (2), and (4)] by

$$\frac{\Delta I(h\nu)}{I_{\text{dark}}} = \sum_{j=1}^k \frac{n_{j,0} - n_j^-(\Phi, t)}{(1 - \beta)n_s}. \tag{5}$$

In order to model the experimentally measured variation of  $\Delta I/I_{\text{dark}}$  with the incident photon dose  $\Phi \cdot t$ , it is necessary to determine the dependence of the filled trap concentrations on illumination time and intensity. This generally requires some consideration of the carrier kinetics during light illumination.

It was shown in Ref. 8 that if recapture of the photoionized carriers is much slower than carrier drift back to the conducting channel, which is an appropriate approximation for these traps,<sup>8</sup> the dependence of the filled trap concentration on illumination time for trap  $j$  is given by

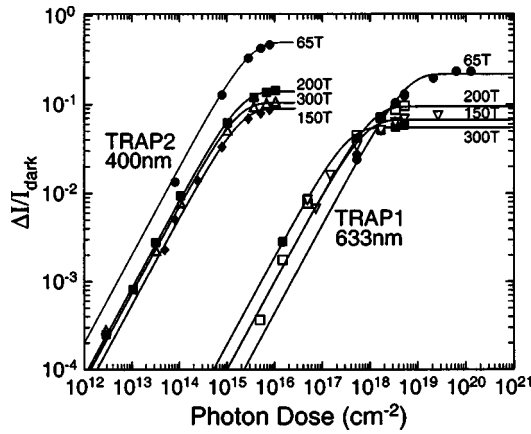


FIG. 2. Dependence of the fractional increase in the drain current on the total light illumination incident on AlGaIn/GaN HEMT devices (After Ref. 13). Data (symbols) was obtained for each of the two traps from devices with HR GaN layers grown at the four different growth pressures indicated, resulting in varying deep trap concentrations. The solid lines are fits to the data using the model.

$$n_j^-(t) = n_{j,0} e^{-\sigma_j(h\nu)\Phi t}, \quad (6)$$

where  $\sigma_j(h\nu)$  is the photoionization cross section of trap  $j$  at the photon energy  $h\nu$  employed in the measurement. This relationship assumes that photoionization events at the various trap species are independent. The dependence of the fractional drain current increase on light illumination then becomes, from Eqs. (3), (5), and (6),

$$\frac{\Delta I}{I_{\text{dark}}} = \sum_{j=1}^k K_j (1 - e^{-\sigma_j(h\nu)\Phi t}), \quad (7)$$

where

$$K_j = \frac{\beta_j}{1 - \beta}. \quad (8)$$

This exponential growth is similar in form to Eq. (22) of Ref. 8, although the  $K_j$  are considerably more complex for the MESFET. Equation (7) may be employed to fit the measured dependence of  $\Delta I/I_{\text{dark}}$  on photon dose. The fitting parameters are the trap photoionization cross sections  $\sigma_j(h\nu)$  and the trap concentrations  $n_{j,0} = \beta_j n_s$  determined from the  $K_j$ .

This fitting procedure was (with minor modification detailed in Sec. III) applied to the data reported in Ref. 13 for four devices with different trap concentrations. The fitted light illumination data are reproduced from Ref. 13 in Fig. 2. Each device was measured at 633 nm, where only one trap is photoionized, and at 400 nm, where both traps are photoionized, so that the two contributions could be separated. The

fitted areal trap concentrations and photoionization cross sections are given in Table I for the four devices, each of which contained different trap concentrations due to intentional variation of the growth pressure of the HR GaN layer during growth by organometallic vapor phase epitaxy.<sup>15</sup> The variations in the trap concentrations were employed in Ref. 13 to correlate the traps with the carbon content in the layers.

The photoionization cross sections,  $\approx 10^{-18} \text{ cm}^2$  for Trap 1 and  $\approx \text{mid-} 10^{-16} \text{ cm}^2$  for Trap 2, are typical<sup>16</sup> for deep defects. It is noteworthy that  $\sigma_j n_{j,0} = \alpha_j d$ , where  $\alpha_j$  is the absorption coefficient associated with photoionization from trap  $j$  and  $d$  is the effective thickness of the layer of charged traps in the HR GaN. From Table I, we find average values for  $\alpha \cdot d$  of  $\approx 4 \times 10^{-4}$  for Trap 2 at 400 nm and  $\approx 1 \times 10^{-6}$  for Trap 1 at 633 nm. With such small absorptions, it would be difficult to obtain spectra such as those in Fig. 1 using conventional optical absorption measurements. The photoionization spectroscopy technique therefore provides a very sensitive method for detecting deep traps in these devices.

### III. EFFECT OF INTERTRAP TRANSITIONS

For the case of two traps, Eq. (7) suggests that the experimental data (Fig. 2) should reflect a single exponential growth function for  $E_1 < h\nu < E_2$  (e.g., Fig. 2, 633 nm), where only a single trap is photoionized, and a superposition of two exponential growth functions for  $h\nu > E_1, E_2$  (e.g., Fig. 2, 400 nm), where both traps are photoionized. The latter case should appear similar to the solid curve in Fig. 3, which represents the superposition of two exponential growth functions (the two dashed curves in the figure). However, this behavior is not observed in the 400 nm data of Fig. 2, which more closely resembles a single exponential growth.

This apparent discrepancy in the 400 nm results occurs because in these devices the photoionization processes at the two trap species are not actually independent. To see this, note first that at the maximum photon dose employed in the 400 nm measurements ( $\approx 1 \times 10^{16} / \text{cm}^2$ ), the collapsed drain current was observed to return to its original value.<sup>13</sup> Since the drain current was fully restored, essentially all Trap 1 and Trap 2 carriers must have been released and returned to the 2DEG. The absence of any indication of superposition in the 400 nm data can only be understood if carriers from the “less-deep” Trap 1 are captured by deeper Trap 2 sites that have been emptied by the incident light, as indicated in the inset in Fig. 3. Because of this coupling between the two trap species, the two photoionization processes are no longer in-

TABLE I. Trap concentrations and photoionization cross sections determined from light illumination measurements of Ref. 13 (shown in Fig. 2) for the two traps responsible for current collapse in these devices.

Device	HR-GaN growth pressure (Torr)	$n_s (10^{12} / \text{cm}^2)$ (Hall effect)	$n_{1,0}$ ( $10^{12} / \text{cm}^2$ )	$n_{2,0}$ ( $10^{12} / \text{cm}^2$ )	$\sigma_1 (633 \text{ nm})$ $10^{-18} \text{ cm}^2$	$\sigma_2 (400 \text{ nm})$ $10^{-16} \text{ cm}^2$
1	65	9.3	1.37	1.74	0.2	4
2	150	12.1	0.74	0.26	1.5	6
3	200	11.5	0.96	0.45	1.1	6
4	300	12.2	0.61	0.55	3.5	8

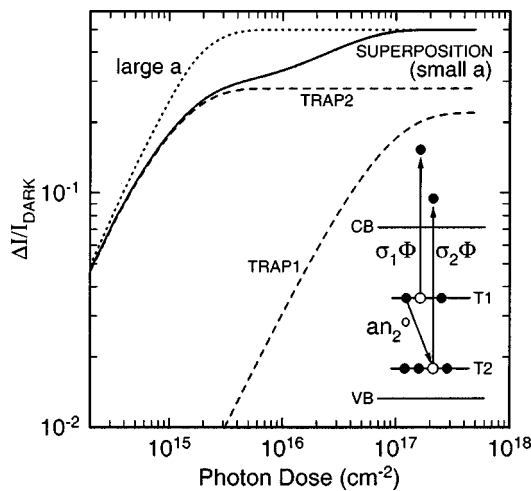


FIG. 3. Simulated results of light illumination studies in an AlGaIn/GaN HEMT structure containing two traps that cause current collapse, with  $h\nu > E_1, E_2$ . The inset describes a level scheme in which transitions from filled Trap 1 sites to empty Trap 2 sites, characterized by the transition rate  $an_2^0(t)$ , compete with the photoionization of Trap 1 carriers, with transition rate  $\sigma_1\Phi$ . For small values of  $a$ , a superposition (solid line) of two independent photoionization processes (two dashed lines) is obtained, similar to the results of Eq. (7). For large  $a$  (dotted line), behavior similar to a single exponential growth function (e.g., 400 nm data in Fig. 2) is observed.

dependent, and Eq. (7) is no longer strictly valid. The Trap 1–Trap 2 transition rate becomes significant *in this case* because: (1) the photoionization cross section  $\sigma_2$  for Trap 2 is relatively large (Table I:  $\approx 10^{-16} - 10^{-15} \text{ cm}^2$ ), so that empty Trap 2 sites necessary to initiate these transitions are created rapidly, and (2) the photoionization cross section for Trap 1 is relatively small ( $\approx 10^{-18} \text{ cm}^2$ ), so the transition rate from Trap 1 to Trap 2 can be comparable or larger than the competing photoionization rate out of Trap 1. Under these conditions, the analysis described in the previous section is modified slightly.

To elucidate this modification, we note first that the curves in Fig. 3 are the result of a numerical simulation (see the Appendix) in which the  $n_j^-(t)$  are calculated by modeling the carrier dynamics of the coupled system shown in the inset of the figure. The photoionization rates,  $\sigma_j\Phi$ , depend on the trap photoionization cross sections and the incident light flux, while the Trap 1–Trap 2 transition rate is proportional to the number of empty Trap 2 sites,  $n_2^0(t) = n_{2,0} - n_2^-(t)$ , through the capture coefficient  $a$  (see Fig. 3 and the Appendix).

Using parameters from device 1 in Table I as an example, the solid curve in Fig. 3 was calculated numerically using a relatively *small* value for the capture coefficient  $a$  ( $1 \times 10^{-13} \text{ cm}^2/\text{s}$ ). This minimizes the importance of Trap 1–Trap 2 transitions, and leads to the straightforward superposition corresponding to Eq. (7). The dotted curve was calculated using a large value for  $a$  ( $1 \times 10^{-10} \text{ cm}^2/\text{s}$ ), and appears similar to single exponential growth, since photoionization out of Trap 1 is essentially “short circuited” by more rapid Trap 1–Trap 2 transitions. This curve is similar to the 400 nm data in Fig. 2. In this case, the carriers from *both* traps are photoionized predominantly through Trap 2. Therefore, for  $h\nu > E_1, E_2$ , the saturation level of  $\Delta I/I_{\text{dark}}$  at

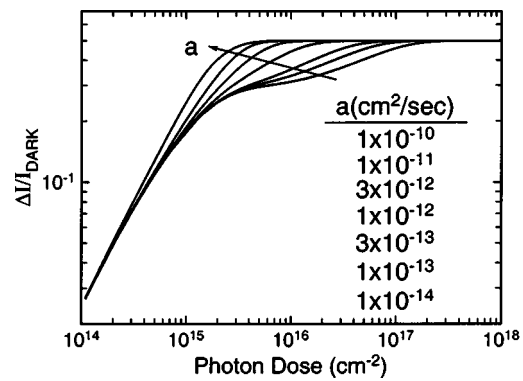


FIG. 4. Effect on simulated light illumination results of varying the capture coefficient  $a$  over a wide range ( $1 \times 10^{-14} - 1 \times 10^{-10} \text{ cm}^2/\text{s}$ ).

large  $\Phi$ , reflected in the fitted value of  $K$ , must correspond to  $(K_1 + K_2)$  rather than  $K_2$ , while the fitted photoionization cross section will be close to that of Trap 2, as observed in the experiment. With this minor modification in the interpretation of the fitting parameter  $K$  for  $h\nu > E_1, E_2$ , the determination of the  $n_{j,0}$  from the fitted  $K$  values [Eqs. (3) and (8)] is straightforward. The effect on the light illumination measurements of varying the capture coefficient  $a$  over a wide range is shown in the simulation in Fig. 4: A continuous change from superposition to single exponential growth is observed.

The particular dependence of the 400 nm data on photon dose observed in Ref. 13 and shown in Fig. 2 occurs because  $\sigma_1 \ll \sigma_2$  and  $\sigma_1\Phi \ll an_2^0(t)$ . A totally different behavior might be expected if different traps with different characteristics were responsible for the current collapse (e.g., devices fabricated using a different growth process or a different material system). For example, if the “less-deep” trap had the larger photoionization cross section, e.g.,  $\sigma_1 \gg \sigma_2$ , we would expect the experiment to reflect a superposition, such as the solid curve in Fig. 3. This follows because  $\sigma_1\Phi \gg an_2^0$ : The carriers at the shallower Trap 1 are photoionized much more rapidly than they can be captured by the few empty deep traps that can be generated with a small  $\sigma_2$ . Whether the light illumination measurements reflect “superposition” or “single exponential growth” for  $h\nu > E_1, E_2$  will therefore depend upon the relative photoionization cross sections of the two traps and the intertrap capture coefficient  $a$ , which should be sensitive to the concentrations of the two trap species.

#### IV. SUMMARY

Photoionization spectroscopy is an effective tool for probing the traps producing current collapse in HEMT devices. In particular, light illumination studies can provide a measure of the photoionization cross sections and the areal concentrations of the traps involved when an appropriate model of the trap photoionization process is available. The model developed here assumes that: (1) current collapse occurs at high drain bias when hot 2DEG carriers are injected into the HR GaN layer, where they are trapped at deep defects, and (2) the drain current increase due to photoionization of the trapped carriers is proportional to the increase in

the sheet charge of the 2DEG. While application of the model to experimental data is straightforward for a single trap species, for two or more traps the analysis requires minor modification. In order to account, for example, for the observed behavior of light illumination measurements where two traps are photoionized simultaneously, transitions from the higher-lying trap to the deepest trap (emptied by photoionization) can play an important role. This occurs when the photoionization rate out of the shallower trap is less than or comparable to the shallow-to-deep trap transition rate.

## ACKNOWLEDGMENTS

The author would like to thank S. Binari and J. Albrecht for a number of very helpful discussions. This work was supported in part by the Office of Naval Research.

## APPENDIX: PHOTOIONIZATION INCLUDING TRAP 1–TRAP 2 TRANSITIONS

With transitions between Trap 1 and Trap 2 included in the model, the dependence of the population of filled traps  $n_j^-(t)$  on illumination time for the level scheme depicted in the inset of Fig. 3 can be determined by solving the two simultaneous differential equations that describe the kinetics for the population of each of the two filled traps. We ignore recapture of the photoionized carriers, as this was found to be a relatively slow process in these materials.<sup>8</sup> The incident photon energy  $h\nu$  is assumed less than both the band gap  $E_g$  and  $E_g - E_A$ , where  $E_A$  is the shallow acceptor binding energy, so that only photoionization from deep traps is considered. The Trap 1–Trap 2 transition rate is proportional to the concentration of empty Trap 2 sites,  $n_2^o(t)$ , through a capture coefficient  $a$ . The dependence of the trap concentrations on illumination time, due to the transitions depicted in Fig. 3, is then described by

$$\frac{dn_1^-(t)}{dt} = -\sigma_1\Phi n_1^-(t) - an_1^-(t)n_2^o(t) \quad (\text{A1})$$

and

$$\frac{dn_2^-(t)}{dt} = -\sigma_2\Phi n_2^-(t) + an_1^-(t)n_2^o(t), \quad (\text{A2})$$

with

$$n_{j,0} = n_j^-(t) + n_j^o(t). \quad (\text{A3})$$

Since all of the traps are filled prior to illumination (i.e., the devices are collapsed), the initial conditions are:  $n_1^-(0) = n_{1,0}$ ,  $n_2^-(0) = n_{2,0}$ . Equations (A1)–(A3) can be solved numerically. The results are illustrated in Fig. 3 using the parameters for device 1 in Table I. The solid curve, calculated using a small value for  $a$  ( $1 \times 10^{-13}$  cm<sup>2</sup>/s), yields a superposition of two essentially independent photoionization processes. The dotted line, calculated using a large value for  $a$  ( $1 \times 10^{-10}$  cm<sup>2</sup>/s), is similar to single exponential growth, as Trap 1 to Trap 2 transitions are enhanced, and most of the trapped carriers are released through photoionization from Trap 2. The effect of varying the parameter  $a$  over a wide range is shown in Fig. 4.

- <sup>1</sup>W. Lu, J. Yang, M. A. Khan, and I. Adesida, *IEEE Trans. Electron Devices* **48**, 581 (2001).
- <sup>2</sup>Y.-F. Wu, D. Kapolnek, J. Ibbetson, P. Parikh, B. P. Keller, and U. K. Mishra, *IEEE Trans. Electron Devices* **48**, 586 (2001).
- <sup>3</sup>S. C. Binari, P. B. Klein, and T. E. Kazior, *Proc. IEEE* **90**, 1048 (2002).
- <sup>4</sup>T. J. Drummond, R. J. Fischer, W. F. Kopp, H. Morkoc, K. Lee, and M. S. Shur, *IEEE Trans. Electron Devices* **30**, 1806 (1983).
- <sup>5</sup>A. Tarakji, G. Simin, N. Ilinskaya, X. Hu, A. Kumar, A. Koudymov, J. Yang, and M. A. Khan, *Appl. Phys. Lett.* **78**, 2169 (2001).
- <sup>6</sup>X. Dang, P. M. Asbeck, E. T. Yu, K. S. Boutros, and J. M. Redwing, *Mater. Res. Soc. Symp. Proc.* **622**, T6.28.1 (2000).
- <sup>7</sup>P. B. Klein, J. A. Freitas, Jr., S. C. Binari, and A. E. Wickenden, *Appl. Phys. Lett.* **75**, 4016 (1999).
- <sup>8</sup>P. B. Klein, S. C. Binari, J. A. Freitas, Jr., and A. E. Wickenden, *J. Appl. Phys.* **88**, 2843 (2000).
- <sup>9</sup>G. Meneghesso, A. Chini, E. Zanoni, M. Manfredi, M. Pavesi, B. Baudart, and C. Gaquiere, *Proceedings of the International Conference on Electronic Materials and Devices*, IEDM 2000 (IEEE, New York, 2000), p. 389.
- <sup>10</sup>M. Wolter, P. Javorka, M. Marso, Aa. Alam, R. Carius, A. Fox, M. Heuken, H. Luth, and P. Kordos, *Proceedings of the International Symposium on Electronic Devices for Microwave and Optoelectronic Applications*, EDMO 2001 (IEEE, New York, 2001), p. 149.
- <sup>11</sup>P. B. Klein, S. C. Binari, K. Ikossi, A. E. Wickenden, D. D. Koleske, and R. L. Henry, *Electron. Lett.* **37**, 661 (2001).
- <sup>12</sup>P. B. Klein, S. C. Binari, K. Ikossi, A. E. Wickenden, D. D. Koleske, and R. L. Henry, *Mater. Res. Soc. Symp. Proc.* **680E**, E5.2.1 (2001).
- <sup>13</sup>P. B. Klein, S. C. Binari, K. Ikossi, A. E. Wickenden, D. D. Koleske, and R. L. Henry, *Appl. Phys. Lett.* **79**, 3527 (2001).
- <sup>14</sup>M. Shur, *Physics of Semiconductor Devices* (Prentice Hall, Englewood Cliffs, N.J., 1990), p. 427.
- <sup>15</sup>A. E. Wickenden, D. D. Koleske, R. L. Henry, R. J. Gorman, M. E. Twigg, M. Fatemi, J. A. Freitas, Jr., and W. J. Moore, *J. Electron. Mater.* **29**, 21 (2000).
- <sup>16</sup>B. K. Ridley, *Quantum Processes in Semiconductors* (Clarendon, Oxford, 1993), p. 184.